Large-Area Supercapacitor Textiles with Novel Hierarchical Conducting Structures

Hao Sun, Songlin Xie, Yiming Li, Yishu Jiang, Xuemei Sun, Bingjie Wang, and Huisheng Peng**

The emergence of wearable electronics has witnessed the rapid advancement of flexible and wearable energy-storage devices in the past decade.[1–6] In particular, supercapacitor textiles on the basis of gel electrolytes share some attractive advantages including high power density, cyclic stability, wearability, safety, and satisfactory energy density, and thus represent promising candidates for next-generation wearable electronics and other applications.[7–21] However, their applications are limited by their low capacitances of typically 10^{-3}–10^{0} F due to their small sizes of several square centimeters. It seems pretty simple to solve the above problem by just increasing the size to enhance the capacitance. Unfortunately, the specific capacitances are largely decreased with the increasing size, despite a lot of effort having been made along this direction. The main problem lies in the fact that the electrodes of supercapacitor textiles are mainly based on carbon nanomaterials and conjugated polymers, which demonstrate relatively low electrical conductivities. The largely increased electrical resistances at large sizes lead to an obvious decrease in energy-storage performance, particularly at high charge/discharge currents.[22,23] On the other hand, metal/graphene hybrid materials have been demonstrated to be efficient as flexible electrodes due to their combined high mechanical and electrical properties, and are promising candidates in various applications such as field-effect transistors.[24–26]

Nature may offer efficient strategies in achieving high performances by creating interesting and useful structures.[27–30] For instance, neural networks are of great importance in effective performance of physiological behavior for biological organisms. Neural signals generated by external stimulation are first collected by the well-distributed peripheral nerves and then transported along trunk nerves to arrive at the brain, and the feedback neural signals work through an inverse process to generate a response. The formed hierarchical networks may also provide inspiration for the development of large-area supercapacitor textiles. If highly conductive trunk pathways are constructed to function as the "trunk nerves", while conductive branches are designed as "peripheral nerves" on a supercapacitor textile, electron collection and transport can be greatly enhanced without the production of high resistances at large sizes.

Here, large-area supercapacitor textiles with high energy-storage performance have been created by designing a hierarchical conducting structure (**Figure 1**a). The current collector grids (CCGs) and graphene-modified fibers are designed to serve as the "trunk nerves" and "peripheral nerves," respectively (Figure 1b). The supercapacitor textiles have been thus scaled up to a size of 100 cm^2 with maintained high specific capacitances, which produce capacitance, power, and energy of 69.3 F, 80.7 mW, and 5.4 mW h, respectively. They are up to four orders of magnitude higher than those in previous reports. The constructed CCG system is also a source of inspiration for

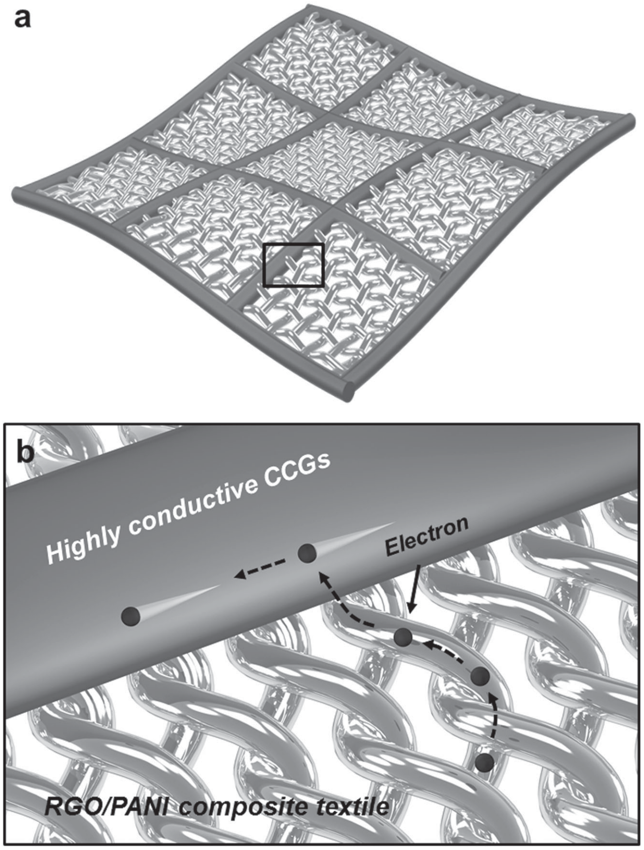

Figure 1. a) Schematic illustration to the large-area textile electrode with a hierarchical conducting structure. b) Schematic illustration of the magnified red rectangle in (a), demonstrating efficient electron transport in the hierarchical conducting structure.

H. Sun, S. Xie, Y. Li, Y. Jiang, Prof. X. Sun, Dr. B. Wang, Prof. H. Peng
State Key Laboratory of Molecular Engineering of Polymers
Department of Macromolecular Science, and Laboratory of Advanced Materials
Fudan University
Shanghai 200438, China
E-mail: wangbingjie@fudan.edu.cn; penghs@fudan.edu.cn

DOI: 10.1002/adma.201602987

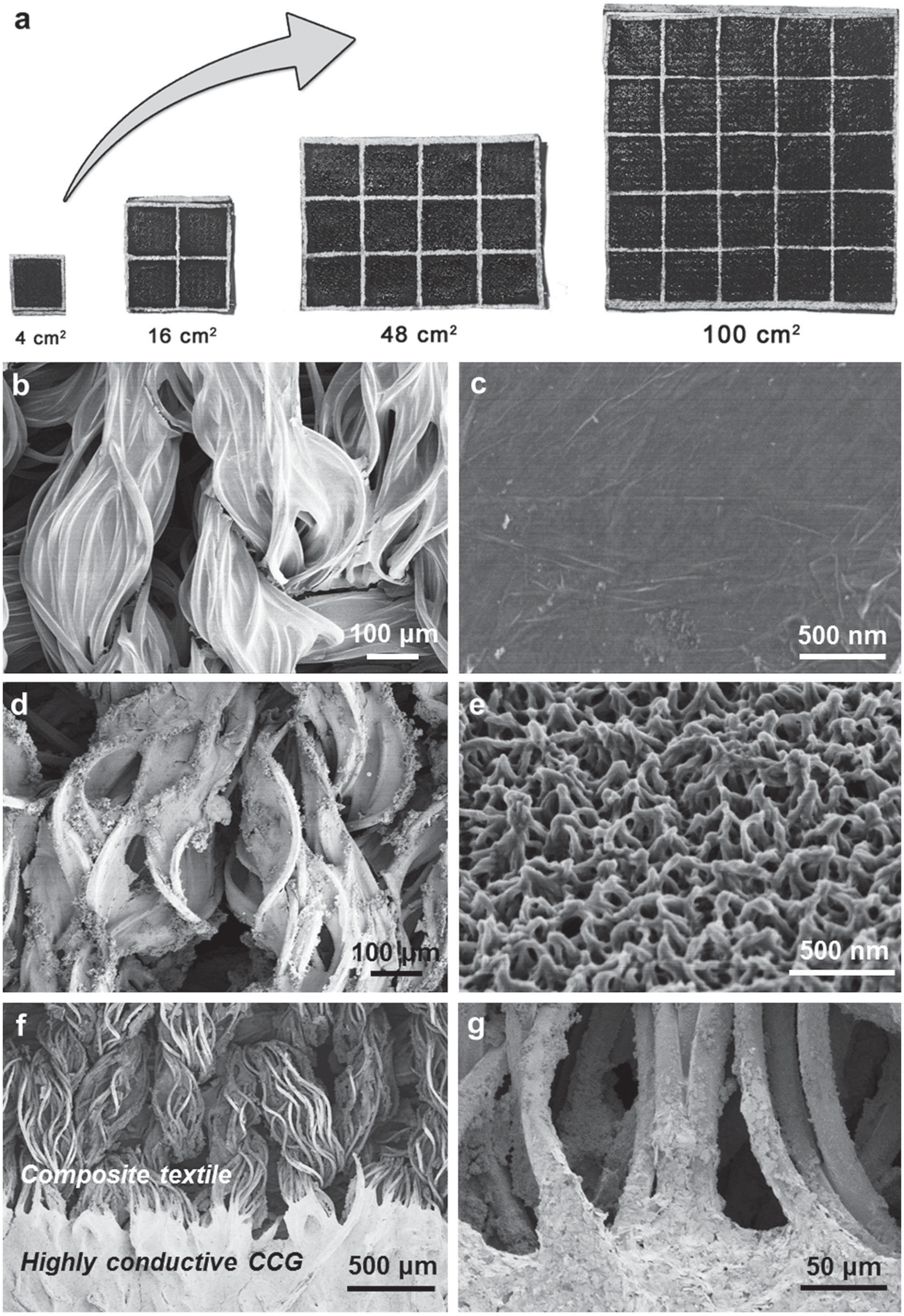

Figure 2. a) Photographs of CCG-based supercapacitor textiles with increasing areas of 4, 16, 48, and 100 cm^2. b,c) SEM images of the RGO/polyester textile electrode at low and high magnifications, respectively. d,e) SEM images of the polyaniline/RGO/polyester textile electrode at low and high magnifications, respectively. f,g) SEM images of the interface between the textile electrode and CCG at low and high magnification, respectively.

developing other textile energy devices, including solar cells and lithium-ion batteries, aiming at high performance.

The supercapacitor textile was prepared through a solution and printing-based process (Figure S1, Supporting Information). Briefly, a polyester textile was immersed into graphene oxide (GO) aqueous dispersion (Figure S2, Supporting Information), and the coated GO sheets were chemically reduced by hydroiodic acid to form a reduced graphene oxide (RGO)/polyester composite textile.[31,32] The high coverage of RGO sheets was verified by Raman spectroscopy, where the sharp peaks for polyester disappeared while the typical D and G bands for RGO appeared (Figure S3, Supporting Information). Polyaniline (PANI) was further incorporated into the RGO/polyester textile via an in situ polymerization,[33,34] followed by screen printing the CCGs on one side of the textile using a commercial silver paste (Figure 1a). A poly(vinyl alcohol) (PVA)/H_3PO_4 gel electrolyte was then coated onto both sides of the textile electrode except the CCG-covered area. The same two modified textile electrodes were stacked with the CCG side at the external surface, and a separator was sandwiched between them to produce a supercapacitor. Due to the scalable preparation methods including dip-coating, in situ polymerization, and screen-printing, the supercapacitor textiles can be readily scaled up, e.g., from 4 to 100 cm^2 (**Figure 2**a).

The formation of high-quality textile electrodes was demonstrated. RGO sheets with sizes of tens of micrometers were closely contacted with the polyester textile substrate (Figure 2b). The resulting RGO-coated polyester fibers had a smooth surface with only a few RGO wrinkles, which verified the formation of a uniform RGO layer (Figure 2c). In particular, the RGO sheets effectively bridged the neighboring polyester fiber, which contributed to a low sheet resistance of ≈150 Ω □$^{-1}$. As a comparison, smaller RGO sheets with sizes of ≈2 µm led to a much higher sheet resistance of ≈3500 Ω □$^{-1}$ as they could not form the above bridged structure. Compared with other carbon nanomaterials, such as carbon nanotube, carbon nanofiber, and other activated carbon nanomaterials, the RGO used in this work demonstrates two advantageous features. On the one hand, due to a better dispersion of GO, large RGO sheets can be uniformly coated onto polyester fibers and form a bridged structure without aggregation, even without the use of surfactants, contributing to a low sheet resistance of the textile electrode. On the other hand, RGO sheets with a 2D configuration provide a better platform for the deposition of the other active materials such as PANI compared with carbon nanotubes and carbon nanofibers in a 1D configuration.[35,36] After the incorporation of PANI, the roughness of the textile had been increased (Figure 2d), and the sheet resistance further decreased to ≈90 Ω □$^{-1}$ due to the formation of more connections among neighboring conducting pathways. The PANI layer demonstrated a porous nanostructure with large specific surface area that could produce high pseudocapacitance (Figure 2e). The incorporation of PANI was further verified by nitrogen-element mapping (Figure S4, Supporting Information). The mass contents were 0.98 and 4.2 mg cm^{-2} for the RGO and PANI, respectively. The close contact between the CCG and textile was also observed (Figure 2f,g) and contributed to the high bending stability of the resulting supercapacitor, which will be discussed later.

Distinguished from the conventional planar supercapacitor using metal foil as the current collector, it was rare to fabricate efficient textile current collectors to reduce the internal resistances, particularly, for a large supercapacitor textile where the electron collection and transport become less efficient. Herein, textile-based CCGs had been designed to overcome the above challenges. On the basis of the hierarchical network structure, the CCGs served as the "trunk nerves" to provide highly conductive pathways for rapid electron transport, contributing to low resistances below 2 Ω between any two points on the CCGs for a 100 cm^2 textile electrode. RGO served as the "peripheral nerves" for efficient electron collection. The dependence of the energy-storage performance on the dimension of the CCGs was first investigated. Sharing the same width of ≈2 mm, CCGs with different dimensions of 10 mm × 10 mm, 15 mm × 15 mm, 20 mm × 20 mm, 25 mm × 25 mm, and 30 mm × 30 mm were produced on five supercapacitor textiles, and the galvanostatic charge–discharge curves were measured at the same

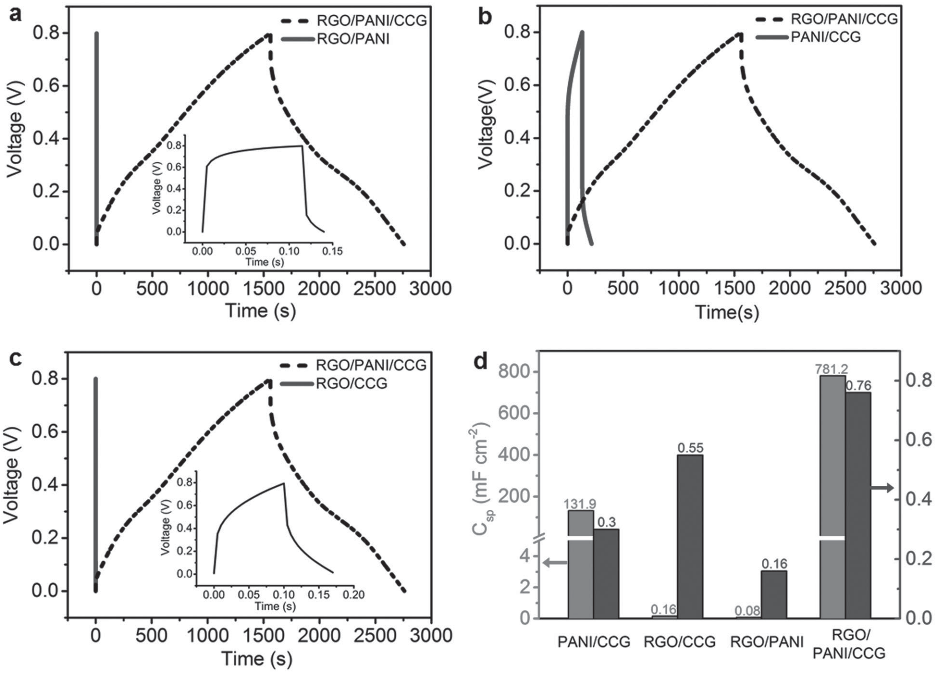

Figure 3. Supercapacitor textiles based on the different electrode materials but with the same area of 16 cm^2 at a current of 8 mA (0.5 mA cm^{-2}). a) Galvanostatic charge–discharge curves with and without CCG (inset, magnified curve). b) Galvanostatic charge–discharge curves with and without RGO. c) Galvanostatic charge–discharge curves with and without PANI (inset, magnified curve). d) Comparison of the specific capacitance and voltage window derived from the galvanostatic charge–discharge curves for different electrode materials.

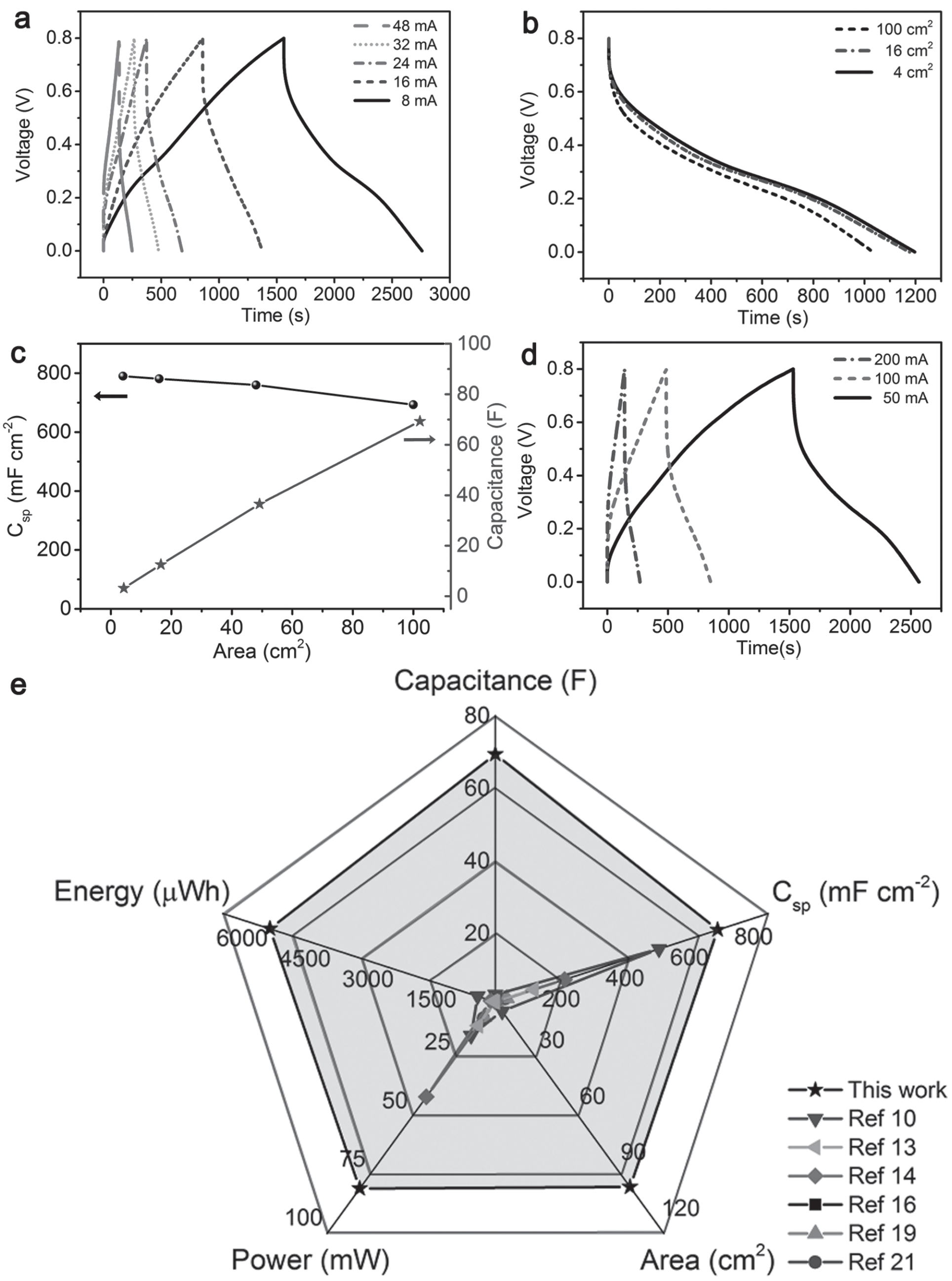

Figure 4. a) Galvanostatic charge–discharge curves of a 16 cm^2 supercapacitor textile at increasing current densities from 0.5 to 3 mA cm^{-2}. b) The galvanostatic discharge curves of supercapacitor textiles with increasing areas from 4 to 100 cm^2 at the same current density of 0.5 mA cm^{-2}. c) Dependence of the specific capacitance and entire capacitance on the area of supercapacitor textile. d) Galvanostatic charge–discharge curves of a 100 cm^2 supercapacitor textile at increasing current from 50 to 200 mA (0.5 to 2 mA cm^{-2}). e) Comparison of the main parameters of this work with the other supercapacitor textiles on the basis of gel electrolyte.[10,13,14,16,19,21] C_{sp} is the specific capacitance of the supercapacitor. Note that the referred performances are all measured in a two-electrode system based on gel electrolyte.

current density of 1 mA cm^{-2} (Figure S5, Supporting Information). The specific capacitance was increased from 608.0 to 755.2 mF cm^{-2} when the dimension first increased from 10 mm × 10 mm to 15 mm × 15 mm, and then slightly decreased to 703.3 mF cm^{-2} at 20 mm × 20 mm, and rapidly decreased to 255.0 mF cm^{-2} at 30 mm × 30 mm due to the insufficient electron transport. A dimension of 20 mm × 20 mm was mainly studied below.

To verify the effectiveness of the designed hierarchical system, the energy-storage performance of the supercapacitor textiles (16 cm^2) without using CCG and RGO was investigated (**Figure 3**). In the absence of the CCG, a low specific capacitance of 0.08 mF cm^{-2} was demonstrated at a current density of 0.5 mA cm^{-2} with a large internal resistance (IR) drop of 0.64 V, indicating a high equivalent series resistance due to the inefficient electron transport (Figure 3a). Without using RGO, a specific capacitance of 131.9 mF cm^{-2} was obtained under the same condition also with a large *IR* drop of 0.5 V, indicating the important role of RGO in enhancing the electron transport during charge–discharge processes (Figure 3b). It was also found that the polyester fibers were separated from each other rather than wrapped together by graphene sheets, and no porous nanostructure of the PANI was observed (Figure S6, Supporting Information). Besides the hierarchical conducting pathways, the high specific capacitance was also attributed to the large pseudocapacitance provided by PANI. As a demonstration, the specific capacitance of a PANI-free supercapacitor textile was measured as 0.16 mF cm^{-2} under the same condition (Figure 3c). Therefore, each component played a critical role in energy storage, and a collective contribution produced the high performance of the supercapacitor textile (Figure 3d).

The electrochemical performance of the supercapacitor textiles with increasing sizes was systematically investigated. For a 16 cm^2 supercapacitor textile, the galvanostatic charge–discharge curves indicated reversible charge–discharge processes at increasing current densities from 0.5 to 3 mA cm^{-2} (currents of 8 to 48 mA) (**Figure 4**a), and the specific capacitance reached 781 mF cm^{-2} at 0.5 mA cm^{-2}. The gravimetric capacitance of the supercapacitor textile was calculated to be 152 F g^{-1} based on the total mass of RGO and PANI, which was comparable or higher than the previous reports.[10,13,16,21] When the size further increased to 100 cm^2, similar discharging times had been shared in the galvanostatic discharge curves at the same current density of 0.5 mA cm^{-2} (Figure 4b), which contributed to a nearly proportional increase of the capacitances (Figure 4c). A 100 cm^2 supercapacitor textile can be normally operated at high charge/discharge currents ranging from 50 to 200 mA (Figure 4d), and a remarkable capacitance of 69.3 F was achieved at 50 mA, which was one to four orders of magnitude higher than that in previous reports (Figure 4e).[10,13,14,16,19,21] Power and energy densities of 807 μW cm^{-2} and 54 μWh cm^{-2} contributed to a high output power and energy of 80.7 mW and 5.4 mW h, respectively (Figure 4e), approaching to the power and energy requirements of many commercial processors, sensors, illuminants, and transmitters. For instance, the energy stored in a 100 cm^2 textile was calculated to be supportable for 412 and 22.5 h standby operation for a commercial electronic watch and wearable wristband, respectively. Even for a mobile phone (Nokia 222-DS), the standby duration reached 12.5 h, indicating the high potential of these supercapacitor textiles in powering next-generation electronic devices with lower-energy-consumption products (**Table 1**). Although these devices can be also powered by small supercapacitors or batteries, large-area supercapacitor textiles show several advantages compared with them. For small supercapacitors, large-area supercapacitor textiles demonstrate longer durations, which are required for practical applications. Despite of the high areal energy densities of small batteries, the generally used organic electrolytes are toxic and evaporable, thus requiring strict encapsulation of the devices, which is particularly difficult for porous textiles. As a comparison, the large-area supercapacitor textiles based on aqueous gel electrolyte demonstrate satisfactory energy density and stability, and the flexibility and wearability are much higher compared with conventional bulky and rigid devices. Besides, the size of the supercapacitor textile can be controlled according to application requirements attributed to the modularized structure. The capacitance of a 16 cm^2 supercapacitor textile can be maintained by 85.9% after 1000 cycles (Figure S7, Supporting Information). A high current density of 10 mA cm^{-2} can be achieved for a 16 cm^2 supercapacitor textile with a CCG size of 10 mm × 10 mm (Figure S8, Supporting Information), contributing to maximal power and energy densities of 2890 μW cm^{-2} and 51 μW h cm^{-2}, respectively.[10,18,21]

Table 1. Calculation of the standby duration for some commercial portable and wearable devices powered by a 100 cm^2 supercapacitor textile. The duration was calculated by dividing the output energy of a 100 cm^2 supercapacitor textile by the standby power of the devices without taking operation voltage into consideration.

Device (Type)	Standby duration [h]
Casio-G-Shock (Electronic watch)	412
Mi Band (Wristband)	22.5
Huawei Honor Band Zero (Wristband)	15.3
Huawei Talk Band B2 (Wristband+Earphone)	11.2
Nokia 222-DS (Mobile phone)	12.5

Considering practical applications, particularly wearable applications of these supercapacitor textiles, heat release represents a critical concern that determines the amenity and safety during use. Therefore, the temperature variation of the supercapacitor textile was traced during galvanostatic charge–discharge processes (**Figure 5**a–d). As expected, the CCG-covered area demonstrated a slightly higher temperature (≈0.8 °C) compared with the other areas on the textile due to a lower resistance. An average temperature of ≈23.5 °C was produced on the entire supercapacitor textile with slight fluctuations during two galvanostatic charge–discharge cycles (Figure 5d), which was demonstrated to be suitable for a variety of wearable applications. Besides, the intrinsic textile feature of the resulting devices promised a stable combination with daily clothes. For instance, a 400 cm^2 supercapacitor textile can be woven into a T-shirt using a commercial sewing machine and demonstrates a superior stability under complex deformations (Figure 5e,f). As an application demonstration, three 100 cm^2 supercapacitor textiles were woven into a T-shirt and connected in-series to serve as a flexible and wearable energy-storage module (Figure 5g). When it was fully charged at a current of 50 mA, the module could light up an “FDU” logo consisting of 44 in-parallel light-emitting diode (LED) lamps even under deformation (Figure 5h).

The large-area supercapacitor textiles demonstrate a variety of advantages that well meet the development trends of next-generation wearable energy-storage systems. First, The solution and printing-based method is favored for continuous and scalable processes in industry. For instance, PANI and RGO were deposited on a polyester T-shirt to make a composite electrode with a large area of ≈7000 cm^2 (Figure S9, Supporting Information). Besides, this work provides a more rapid deposition of PANI and lower electrical resistance of the textile electrode compared with another report.[20] Second, it was highly flexible and conformable to even irregular substrates (Figure S10 and S11, Supporting Information). The capacitance was well maintained under bending with increasing angles (Figure S12, Supporting Information), and 95.6% of the initial value was maintained

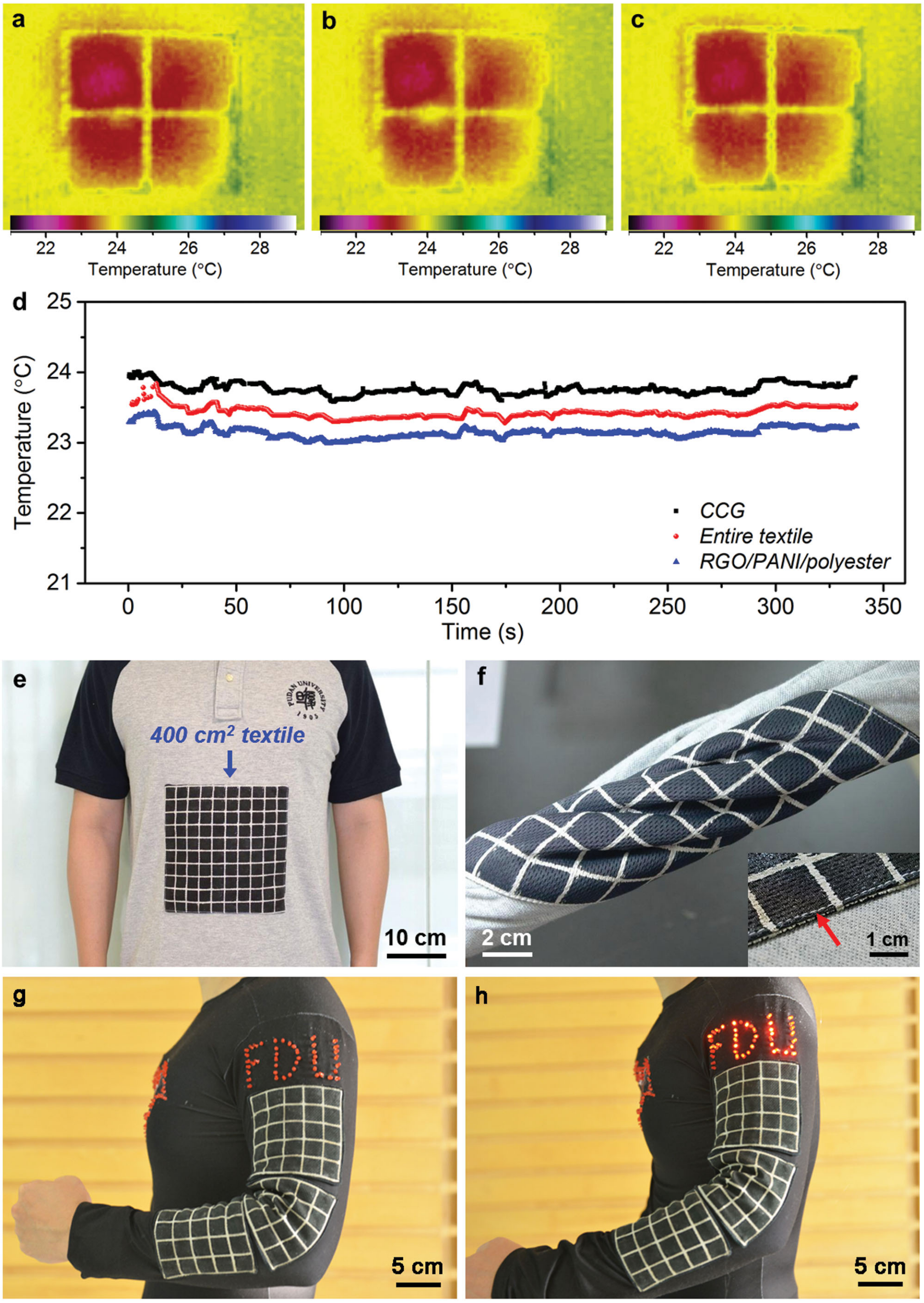

Figure 5. a–c) Infrared camera images of a supercapacitor textile at the beginning, middle, and end of a galvanostatic charge–discharge cycle. d) Temperature variations of the CCG, PANI/RGO, and entire device during two galvanostatic charge–discharge cycles at a current density of 4 mA cm^{-2}. e,f) Photographs of a 400 cm^2 supercapacitor textile woven into a T-shirt (e) and under deformation (f). The photograph in the inset in (f) shows the weaving interface between the supercapacitor textile and T-shirt. g,h) Photographs of three in-series supercapacitor textiles (100 cm^2 each) woven into a T-shirt (g), and successfully lit up an "FDU" logo consisting of 44 red LED lamps under deformation (h).

after continuous bending at 90° for 1000 cycles (Figure S13, Supporting Information). Third, the aqueous gel electrolyte is safer and more stable compared with organic or liquid counterparts. Fourth, compared with the conventional method through the use of conducting wires or foils to connect small-sized supercapacitor textiles together, the hierarchical conducting structure demonstrates higher integrity, flexibility, and stability and reduces the technical complexity, production cost, and contact resistances, which well meets the trends of integration and modularization in modern electronics. Last but not the least, the novel hierarchical conducting structure represents a general and effective strategy in scaling up a variety of electronic devices. It should be noted that the development of small-area supercapacitor textiles with high areal capacitances and energy densities represents another strategy for some specific applications and can be also served as the building blocks for large-area supercapacitor textiles.[7,9,11,12]

A variety of nanomaterials has been used to improve the supercapacitor textiles. However, there remains a key challenge in inefficient charge transport at nanomaterial-based electrodes, which in fact also exists for other electronic devices. Here, the hierarchical conducting structure represents a promising strategy in solving the above problem. First, the CCGs serve as conducting pathways and PANI/RGO components enhance both charge transport and specific capacitance. Second, large RGO sheets form bridges among polyester fibers with fewer boundaries and lower electrical resistances. It is well known that the electrical resistance mainly comes from the contact resistances among nanomaterials. Third, the good interfaces derived from the close contacts between the CCG and PANI/RGO modified fiber and between RGO and PANI based on hydrogen bonds and π–π interactions favor charge transport.

In summary, aiming at a practical application, a novel family of large supercapacitor textiles has been developed with high-energy-storage performance, inspired by the hierarchical neural-network structure. The design of the CCG system makes it effective to reach an effective large area of 100 cm^2 with high capacitance, power, and energy of 69.3 F, 80.7 mW, and 5.4 mW h, respectively, which is up to four orders of magnitude higher, compared with those in previous reports. The resulting supercapacitor textiles are also flexible and wearable, which is required for many emerging applications, such as wearable electronics and smart clothes. This work also offers a new platform in the advancement of high-performance flexible energy harvesting and storage devices.

Experimental Section

Synthesis of Graphene Oxide (GO): The GO was prepared via a modified Hummer's method.[37] Large and small GO sheets were prepared from flake graphite powders with average lateral sizes of 300 and 38 µm, respectively. 5 g of flake graphite powder was added to a mixture of 150 mL of sulfuric acid and 50 mL of nitric acid, followed by stirring for 24 h. After repeatedly filtrating and washing with deionized water to remove the residual acid, the obtained expandable graphite was exfoliated in a tube furnace at 1000 °C for 10 s, followed by mixing with 300 mL of oleum, 4.2 g of $K_2S_2O_8$, and 6.2 g of P_2O_5 successively and reacted at 80 °C for 5 h under continuous stirring. After cooling down to room temperature, the suspension was diluted with 2 L of deionized water, followed by vacuum filtrating and washing for three times. The dried powder was then added to 200 mL of oleum in an ice bath under stirring, followed by slowly adding 15 g of $KMnO_4$ under vigorous mechanical stirring with the temperature controlled below 20 °C. The reactants were then heated to 35 °C and stirred for 2 h, followed by diluting with 2 L of deionized water and adding 10 mL of 30 wt% H_2O_2 to remove the residual permanganate and MnO_2. The dispersion was then left overnight, and the bottom gel was washed with deionized water, followed by centrifugation for five times with the addition of 1 M HCl solution and washing with deionized water until the decantate became nearly neutral. The resulting gel was diluted with deionized water and ultrasonicated to obtain well-dispersed GO solution.

Preparation of PANI/RGO/Polyester Textile Electrodes: A polyester textile (thickness, ≈1 mm, J-2284) was dipped into a well-dispersed GO solution (≈2 mg mL^{-1}) and was dried at 100 °C for ≈10 min. The above process was repeated for five times to increase the loading mass of GO, followed by the reduction of GO in HI aqueous solution (40 wt%) at 80 °C for 6 h.[31,32] The modified polyester textile was then washed with deionized water twice and then dried in air. For the in situ deposition of PANI, the resulting polyester textile was first immersed into the mixture of 0.5 M aniline and 1 M HCl at 35 °C for 2 h to enhance the permeation of aniline monomers into the textile. After dropwise addition of a mixture of 0.5 M $(NH_4)_2S_2O_8$ and 1 M HCl, the reaction was kept at 0 °C for 30 min,[33,34] followed by washing with deionized water and drying to obtain the PANI/RGO/polyester textile electrode.

Fabrication of Current Collector Grid (CCG)-Based Supercapacitor Textiles: The CCGs were screen-printed onto one side of a textile electrode using a commercial silver paste (SC666-80R, Uniwell) and then dried at 80 °C for 1 h. Two textile electrodes were coated with PVA/H_3PO_4 gel electrolyte (mass ratio of 1/1) on both sides except the CCG-covered area, followed by vacuum treatment to enhance the permeation of gel electrolyte into the textile electrode. The two textile electrodes were then stacked together with the CCG side on the external surface, and a separator (TF4030, NKK) was sandwiched between them to prevent short-circuiting.

Calculation of the Electrochemical Parameter: The capacitance (C) was calculated from the equation of $C = (I \times \Delta t)/\Delta V$, where I, Δt, and ΔV correspond to the discharge current, discharge time, and voltage window, respectively. The specific areal capacitance the supercapacitor textile was calculated by dividing the capacitance by the area of the supercapacitor textile. The gravimetric capacitance of the supercapacitor textile was calculated by dividing the capacitance by the total mass of RGO and PANI on two textile electrodes. The energy (E) was calculated from the equation of $E = C \times \Delta V^2/(2 \times 3600)$. The power ($P$) was calculated from the equation of $P = E \times 3600/\Delta t$. The energy density ($E_A$) and power density ($P_A$) were calculated by dividing the energy and power by the area of the supercapacitor textile, respectively.

Supporting Information

Supporting Information is available from the Wiley Online Library or from the author.

Acknowledgements

H.S. and S.X. contributed equally to this work. This work was supported by NSFC (21225417, 51573027, 51403038), STCSM (15XD1500400, 15JC1490200), and the Program for Outstanding Young Scholars from Organization Department of the CPC Central Committee.

Received: June 6, 2016
Revised: July 5, 2016

---

[1] Z. Yang, J. Deng, X. Chen, J. Ren, H. Peng, *Angew. Chem., Int. Ed.* **2013**, *52*, 13453.
[2] Z. Niu, L. Zhang, L. Liu, B. Zhu, H. Dong, X. Chen, *Adv. Mater.* **2013**, *25*, 4035.
[3] D. Yu, K. Goh, H. Wang, L. Wei, W. Jiang, Q. Zhang, L. Dai, Y. Chen, *Nat. Nanotechnol.* **2014**, *9*, 555.
[4] D. Yu, S. Zhai, W. Jiang, K. Goh, L. Wei, X. Chen, R. Jiang, Y. Chen, *Adv. Mater.* **2015**, *27*, 4895.
[5] L. Kou, T. Huang, B. Zheng, Y. Han, X. Zhao, K. Gopalsamy, H. Sun, C. Gao, *Nat. Commun.* **2014**, *5*, 3754.
[6] M. Yu, Y. Han, X. Cheng, L. Hu, Y. Zeng, M. Chen, F. Cheng, X. Lu, Y. Tong, *Adv. Mater.* **2015**, *27*, 3085.
[7] L. Hu, M. Pasta, F. L. Mantia, L. Cui, S. Jeong, H. D. Deshazer, J. W. Choi, S. M. Han, Y. Cui, *Nano Lett.* **2010**, *10*, 708.
[8] G. Yu, L. Hu, M. Vosgueritchian, H. Wang, X. Xie, J. R. McDonough, X. Cui, Y. Cui, Z. Bao, *Nano Lett.* **2011**, *11*, 2905.
[9] L. Bao, X. Li, *Adv. Mater.* **2012**, *24*, 3246.

[10] K. Jost, D. Stenger, C. R. Perez, J. K. McDonough, K. Lian, Y. Gogotsi, G. Dion, *Energy Environ. Sci.* **2013**, *6*, 2698.
[11] K. Jost, C. R. Perez, J. K. McDonough, V. Presser, M. Heon, G. Dion, Y. Gogotsi, *Energy Environ. Sci.* **2011**, *4*, 5060.
[12] L. Dong, C. Xu, Y. Li, C. Wu, B. Jiang, Q. Yang, E. Zhou, F. Kang, Q. H. Yang, *Adv. Mater.* **2016**, *28*, 1675.
[13] P. Yang, Y. Ding, Z. Lin, Z. Chen, Y. Li, P. Qiang, M. Ebrahimi, W. Mai, C. P. Wong, Z. L. Wang, *Nano Lett.* **2014**, *14*, 731.
[14] X. Xiao, T. Ding, L. Yuan, Y. Shen, Q. Zhong, X. Zhang, Y. Cao, B. Hu, T. Zhai, L. Gong, J. Chen, Y. Tong, J. Zhou, Z. L. Wang, *Adv. Energy Mater.* **2012**, *2*, 1328.
[15] S. Pan, H. Lin, J. Deng, P. Chen, X. Chen, Z. Yang, H. Peng, *Adv. Energy Mater.* **2015**, *5*, 1401438.
[16] T. G. Yun, B. i. Hwang, D. Kim, S. Hyun, S. M. Han, *ACS Appl. Mater. Interfaces* **2015**, *7*, 9228.
[17] Y. Meng, Y. Zhao, C. Hu, H. Cheng, Y. Hu, Z. Zhang, G. Shi, L. Qu, *Adv. Mater.* **2013**, *25*, 2326.
[18] H. Cheng, Z. Dong, C. Hu, Y. Zhao, Y. Hu, L. Qu, N. Chen, L. Dai, *Nanoscale* **2013**, *5*, 3428.
[19] G. Wang, H. Wang, X. Lu, Y. Ling, M. Yu, T. Zhai, Y. Tong, Y. Li, *Adv. Mater.* **2014**, *26*, 2676.
[20] F. Shao, S. Bian, Q. Zhu, M. Guo, S. Liu, Y. Peng, *Chem. Asian J.* **2016**, *11*, 1906.
[21] K. Jo, C. H. Kim, S. Won, Y. Hwangbo, J. H. Kim, H. J. Lee, S. M. Lee, *J. Mater. Chem. A* **2016**, *4*, 4082.
[22] J. Xu, D. Wang, Y. Yuan, W. Wei, L. Duan, L. Wang, H. Bao, W. Xu, *Org. Electron.* **2015**, *24*, 153.
[23] W. Li, C. Mak, C. Kan, C. Hui, *RSC Adv.* **2014**, *4*, 64890.
[24] M. S. Lee, K. Lee, S. Y. Kim, H. Lee, J. Park, K. H. Choi, H. K. Kim, D. G. Kim, D. Y. Lee, S. Nam, J. U. Park. *Nano Lett.* **2013**, *13*, 2814.
[25] B. W. An, B. G. Hyun, S. Y. Kim, M. Kim, M. S. Lee, K. Lee, J. B. Koo, H. Y. Chu, B. S. Bae, J. U. Park, *Nano Lett.* **2014**, *14*, 6322.
[26] J. Kim, M. S. Lee, S. Jeon, M. Kim, S. Kim, K. Kim, F. Bien, S. Y. Hong, J. U. Park, *Adv. Mater.* **2015**, *27*, 3292.
[27] Y. Zheng, H. Bai, Z. Huang, X. Tian, F. Q. Nie, Y. Zhao, J. Zhai, L. Jiang, *Nature* **2010**, *463*, 640.
[28] H. Chen, P. Zhang, L. Zhang, H. Liu, Y. Jiang, D. Zhang, Z. Han, L. Jiang, *Nature* **2016**, *532*, 85.
[29] K. Y. Ma, P. Chirarattananon, S. B. Fuller, R. J. Wood, *Science* **2013**, *340*, 603.
[30] H. Sun, X. Fu, S. Xie, Y. Jiang, H. Peng, *Adv. Mater.* **2016**, *28*, 2070.
[31] S. Pei, J. Zhao, J. Du, W. Ren, H. M. Cheng, *Carbon.* **2010**, *48*, 4466.
[32] J. Zhao, S. Pei, W. Ren, L. Gao, H. M. Cheng, *ACS Nano* **2010**, *4*, 5245.
[33] N. R. Chiou, C. Lu, J. Guan, L. J. Lee, A. J. Epstein, *Nat. Nanotechnol.* **2007**, *2*, 354.
[34] Y. Wang, H. Li, Y. Xia, *Adv. Mater.* **2006**, *18*, 2619.
[35] H. Wang, Q. Hao, X. Yang, L. Lu, X. Wang, *ACS Appl. Mater. Inter.* **2010**, *2*, 821.
[36] Z. Yang, H. Sun, T. Chen, L. Qiu, Y. Luo, H. Peng, *Angew. Chem., Int. Ed.* **2013**, *52*, 7545.
[37] Z. Xu, H. Sun, X. Zhao, C. Gao, *Adv. Mater.* **2013**, *25*, 188.